International Biodeterioration & Biodegradation 209 (2026) 106296

Contents lists available at ScienceDirect

International Biodeterioration & Biodegradation

journal homepage: www.elsevier.com/locate/ibiod

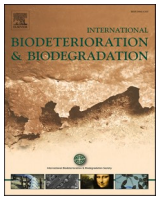

Moisture dynamics during *Coniophora puteana* brown rot degradation of Scots pine sapwood

Tiina Belt [a], Andreas Treu [b], Veikko Möttönen [a], Michael Altgen [b,*]

[a] Natural Resources Institute Finland, Production Systems, Viikinkaari 9, 00790, Helsinki, Finland
[b] Norwegian Institute of Bioeconomy Research, Department of Wood Technology, P.O. Box 115, 1431, Ås, Norway

ARTICLE INFO

Keywords:
Bound water
brown rot
Decay
Hygroscopicity
LFNMR
Moisture content
Sorption

ABSTRACT

Wood has many attractive material qualities, but it is susceptible to biological degradation by wood-decaying fungi. Moisture is one of the critical requirements for wood decay, but much remains unknown about moisture dynamics in decaying wood. To fill this knowledge gap, this study investigated moisture in Scots pine sapwood during decay caused by the brown rot fungus *Coniophora puteana*. Samples were exposed to decay in two time-series experiments; mass loss and moisture content were recorded over the course of decay, and the bound and free water populations in the samples were analysed using low-field nuclear magnetic resonance (LFNMR) relaxometry in both the decaying state and at full water saturation. Selected samples were also used for water vapour sorption measurements. The time-series decay tests showed that moisture content initially increased due to fungal activity but decreased over time when corrected for mass loss, contrary to the general belief that moisture content increases with decay. LFNMR revealed that bound water content increased on a decayed-mass basis in the decaying state and at saturation, but no increase was seen after correction for mass loss. Free water content followed gravimetric moisture content in the decaying state, but the saturated state measurements revealed an initial increase and subsequent decrease with mass loss. Degradation caused changes in hygroscopicity, but our data show that overall moisture content is regulated by fungal activity rather than by material properties. These findings highlight the complexity of water interactions during fungal degradation, offering valuable new insights into wood degradation mechanisms.

1. Introduction

Wood has many positive attributes as a building material, such as renewability, carbon sequestration, and a high strength-to-mass ratio (Wimmers, 2017). However, as a natural material, wood is susceptible to biological degradation. One of the most destructive forms of degradation in terrestrial environments is caused by wood-decaying fungi, which are traditionally classified as brown rot, white rot, and soft rot (Zabel and Morrell, 2020). Brown rot decay is caused by basidiomycetes and is characterised by the preferential degradation of wood cell wall carbohydrates, which leaves behind a residue of modified lignin (Arantes and Goodell, 2014). Although brown rot fungi account for less than 10% of all wood-decaying basidiomycetes (Arantes and Goodell, 2014), they are the most commonly identified wood-decaying fungi in buildings, at least in Europe and North America, where the occurrence of fungi in buildings has been documented (Gabriel and Švec, 2017; Schmidt, 2007).

As living organisms, wood-decaying fungi have specific physiological requirements. The amount of moisture in the wood material is one of the most critical requirements and one that has been extensively studied (Brischke and Alfredsen, 2020). It is often stated that decay initiation and development require free water, which can exist in wood under high moisture conditions when the cell walls are or are close to being saturated (Fredriksson, 2019; Fredriksson and Thybring, 2019). When the surrounding air is the only source of moisture in wood, the initiation of brown rot decay appears to be limited to 95-100% RH (e.g. Brischke et al., 2017; Viitanen et al., 2010), at which point free water may or may not exist. In the presence of an additional moisture supply, however, decay can sometimes be initiated at wood moisture contents well below cell wall saturation (Meyer and Brischke, 2015; Stienen et al., 2014). Local moisture content differences have been found in wood exposed to fungi (Hiltunen et al., 2020; Müller et al., 2001), indicating that free water may be present locally even in drier samples. Alternatively, free water might not be required for decay. As reviewed by Jakes et al. (2019), it was previously thought that aqueous pathways needed to

* Corresponding author.
E-mail address: michael.altgen@nibio.no (M. Altgen).

https://doi.org/10.1016/j.ibiod.2026.106296
Received 6 October 2025; Received in revised form 3 February 2026; Accepted 4 February 2026
Available online 5 February 2026

form within the wood cell walls to allow for the diffusion of ions and other solutes. However, recent scientific approaches describe it as diffusion through a solid polymer matrix, promoted by water plasticisation but not requiring cell wall water saturation (Jakes et al., 2019).

After initiation, wood moisture content is believed to increase with the progression of decay because carbohydrate breakdown by fungi generates water (Thybring, 2017). However, very few studies have reported moisture contents in decaying wood over the course of decay. Saito et al. (2012) reported an increase in gravimetric moisture content with increasing mass loss; however, the data were not corrected for mass loss, and the increase was largely due to a decrease in wood mass rather than an increase in water mass. Other studies reported highly variable values (Cardias, 1992; Cardias Williams and Hale, 2003). In addition to an overall increase in moisture content, brown rot decay may also increase the amount of bound water in the wood cell walls. The removal of carbohydrates from the cell wall is expected to increase porosity and create new water-accessible cell wall space (Thybring, 2017), which may be occupied by water under favourable conditions. Brown rot degradation has indeed been shown to increase cell wall water-holding capacity at full water saturation (Belt and Altgen, 2025; Flournoy et al., 1991), although Belt and Altgen (2025) found that water capacity increased only in the early stages of decay when corrected for mass loss. Brown rot degradation has also been shown to increase in hygroscopicity when measured before drying (Belt et al., 2024; Belt and Altgen, 2025), which may further contribute to an increase in bound water. However, no studies have investigated changes in bound water content in the decaying state.

The uncertainties related to fungal water requirements and the states of water in wood call for more studies on water in wood during fungal decay, using methods that can distinguish between different water populations. One method for obtaining information on different water populations in wood is low-field nuclear magnetic resonance (LFNMR) relaxometry, which measures the relaxation of water-bound hydrogen nuclei after a radio frequency pulse (Fredriksson and Thygesen, 2017). Different water populations have distinct relaxation times, which can be used to distinguish between water populations in various chemical and physical environments. LFNMR has been used to study water in unmodified and modified wood at full saturation (e.g. Beck et al., 2018b; Fredriksson and Thygesen, 2017; Thybring et al., 2020; Yang et al., 2020) and at various moisture states above and below cell wall saturation (Almeida et al., 2007; Araujo et al., 1992; Bonnet et al., 2017; Cox et al., 2010; Fredriksson et al., 2024; Fredriksson and Thybring, 2019; Müller et al., 2001; Sun et al., 2024; Telkki et al., 2013; Thygesen and Elder, 2008). It has also been used to study changes in wood-water interactions in brown rot degraded wood (Beck et al., 2018a; Hiltunen et al., 2020), but it has not been used to analyse water in wood during fungal degradation.

The objective of the present study is to determine how overall, bound, and free moisture content change as brown-rot decay by *Coniophora puteana* progresses in Scots pine (*Pinus sylvestris*) and whether these moisture dynamics are affected by material properties.

2. Materials and methods

2.1. Sample preparation

Scots pine (*Pinus sylvestris* L.) was chosen as the wood species because water populations in softwood species are well described in previous LFMR studies (e.g. Beck et al., 2018b, 2018a; Fredriksson and Thygesen, 2017; Telkki et al., 2013) and because its sapwood is very susceptible to fungal decay (EN 350, 2016). Small cylindrical samples (6 mm diameter, 10 mm length) were prepared from Scots pine sapwood boards by cutting them in the transverse direction into 10 mm thick slices from which the samples were punched out using a steel hole punch. Thereby, the length of the cylindrical samples was oriented along the fibre direction. The wood material was sampled from a forest in Østfold County, Norway (59° 33′ 1.453″ N, 10° 53′ 31.437” E), and the wood species identification was confirmed based on the anatomical features described by Richter et al. (2004). The samples used for decay test 1 had an average undecayed mass of 0.21 g, while the samples used for test 2 had an average undecayed mass of 0.15 g. All samples selected for decay tests were free of knots and visible defects. The samples were dried at 105 °C for 24 h, weighed to determine their initial dry mass, and conditioned at 85% RH over a saturated solution of KCl for 3-5 weeks. Finally, the samples were wrapped in aluminium foil and sterilised by autoclaving (2 × 20 min) immediately before the start of the decay tests.

2.2. Time-series decay tests

The prepared samples were exposed to decay by the brown rot fungus *Coniophora puteana* (Schumach.: Fr.) P. Karst., one of the most commonly reported decay fungi in buildings (Gabriel and Švec, 2017; Schmidt, 2007). Two decay tests were performed; decay test 2 was established to verify the results obtained from decay test 1 and was run at a later time with minor modifications to the test method. Both decay tests were time-series experiments with five harvest time points: 1, 2, 3, 4, and 5 weeks. Decay test 2 also had an additional time 0 point, which comprised samples harvested immediately after sterilisation. The decay tests were conducted in screw-cap plastic jars (110 mm diameter, 750 ml total volume). The jars contained 70 ml of 2% malt extract agar and had caps with one 16 mm hole plugged with cotton wool for gas exchange. The jars were inoculated with one plug of *C. puteana* (strain BAM Ebw. 15, Bundesanstalt für Materialforschung und -prüfung, BAM, Germany) from malt extract agar stock cultures or left uninoculated to produce sterile control jars. Two inoculated jars and one control jar without fungal inoculum were prepared for each time point and decay test, and incubated at room conditions until the mycelium covered the agar surface in the inoculated jars. The sterilised wood samples were then added to the jars over plastic mesh supports to separate them from the agar medium. Each inoculated jar received five sterilised wood samples (for a total of ten replicates per time point per test), while the control jars received ten samples each (total of ten replicates per time point per test). The inoculated and control jars were incubated at room temperature for 1, 2, 3, 4, or 5 weeks. The decay test 1 jars were incubated at 85% RH over a saturated solution of KCl, while the decay test 2 jars were incubated at ambient RH (<50 % RH). After incubation, the decayed and control samples were removed from the jars, wiped to remove adhered mycelium, weighed to determine their decaying wet mass, and individually sealed in tightly-wrapped plastic. The samples were processed as rapidly as possible, one at a time, to prevent moisture loss. The wrapped samples were stored in the freezer at −20 °C until they were transported to the low-field nuclear magnetic resonance (LFNMR) analysis. The decay test setup and subsequent analyses are summarised in Fig. 1.

2.3. LFNMR

The decay test samples were first measured in the decaying condition. All decayed samples (weeks 1-5, N = 10) and selected control samples (weeks 1 and 5 from decay test 1, N = 10; time 0 and week 5 from decay test 2, N = 10) were measured. The samples were equilibrated at room temperature (23 °C) while still in their plastic wrapping. Afterwards, they were individually removed from the wrapping, weighed to determine moisture loss during storage and transport, placed in a glass NMR tube, and measured at 23 °C. They were then weighed again to determine moisture loss during measurement. After the decaying state measurement, the samples from test 2 were water-saturated. They were individually placed in water-filled 2 ml plastic tubes and vacuum impregnated for ca. 15 min. After ca. 40 h of incubation under ambient conditions, the samples were measured in the water-saturated condition. They were individually removed from their plastic tubes, and excess water at the surface was removed using moist

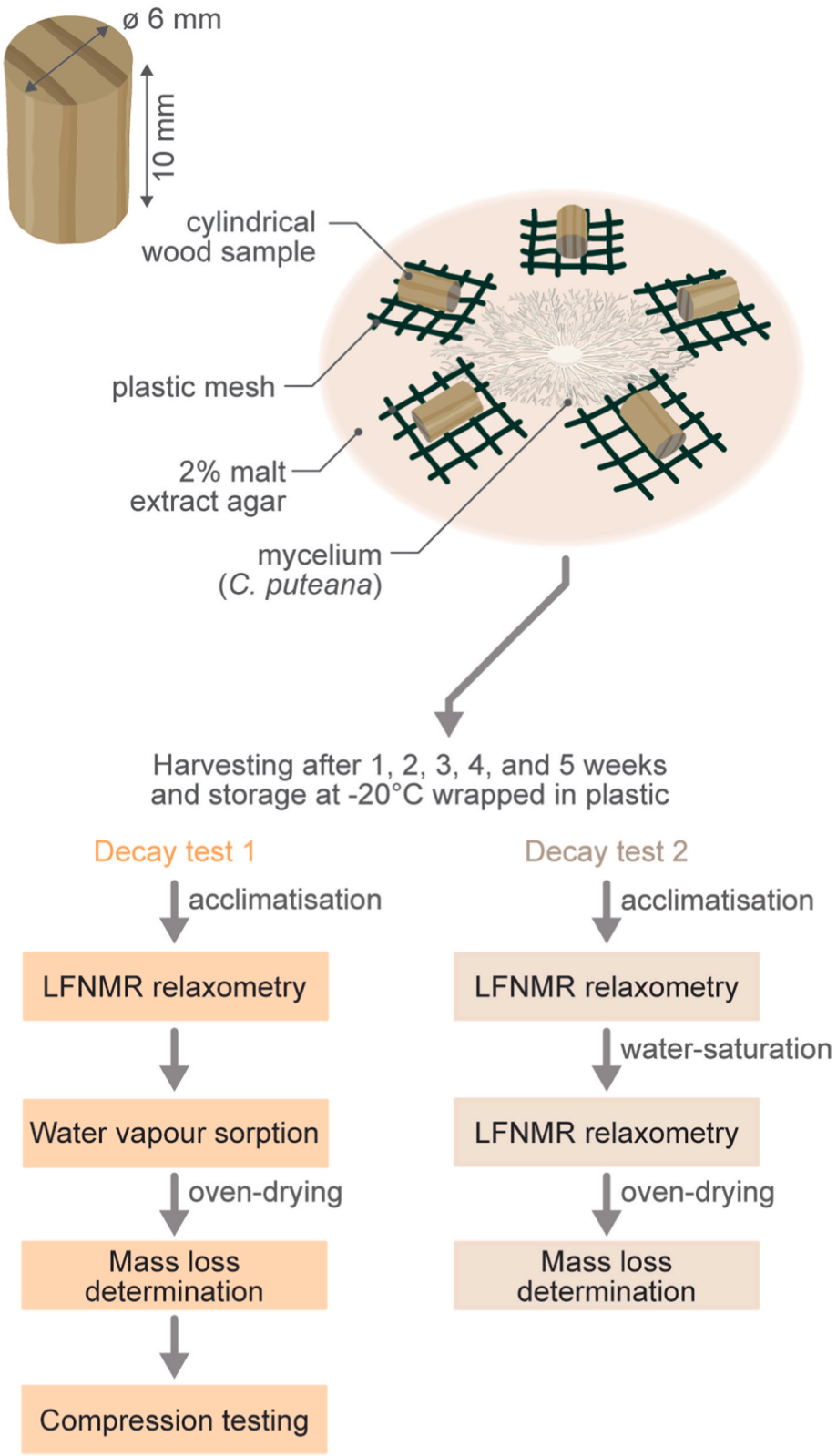

Fig. 1. Summary of the decay test setup and the subsequent analyses. Additional sterile control samples were incubated under decay test conditions in the absence of fungus and used for subsequent analyses alongside the decayed samples.

tissue paper. The samples were first weighed to determine their saturated moisture content, then placed in a glass NMR tube and measured at 23 °C, and finally weighed again to determine moisture loss during measurement. Average moisture losses during sample handling (transport, decaying state measurement, saturated state measurement) are shown in Supplementary Fig. S1.

All LFNMR measurements were performed on a Bruker mq20 Mini spec spectrometer (Bruker, Billerica, MA, USA) with a 0.47 T permanent magnet. A Bruker BVT 3000 nitrogen temperature control unit was used to maintain the temperature. Spin-spin relaxation time (T_2)

measurements were performed using a 1D Carr–Purcell–Meiboom–Gill (CPMG) pulse sequence (Carr and Purcell, 1954; Meiboom and Gill, 1958) with a 0.04 ms pulse separation, 32 000 echoes, 16 scans, and a 10 s recycle delay. The gain was tuned for the wettest samples and kept constant at 75 dB throughout the measurements. The CPMG decay curves were analysed using inverse Laplace transformation via the MATLAB code constructed by Godefroy et al. (2003), with the regularised non-negative least squares (NNLS) method. This transforms the decay curve into a continuous distribution of T_2 values. The range for the distribution was set to 0.09–700 ms with 200 data points. In the regularised NNLS fitting, the smoothing parameter α has a strong influence on the resulting relaxation time distributions. Following Godefroy et al. (2003), the α value was chosen based on a chi-squared (χ^2) distribution with χ^2 as a function of α. The optimal α value results in a distribution that is least sensitive to random noise, avoiding over-smoothing that could merge otherwise separated peaks (low α value) as well as an ill-posed problem (high α value). In this experiment, the optimal α value was 10^{10} for most measurements or between 10^{10} and 10^{11} for a small number of measurements. For consistency, the α value was set to 10^{10} for all measurements. For quantitative analysis of the LFNMR data, the peaks on the relaxation time distributions were identified, and their areas and peak times (T_2 values corresponding to maximum peak intensity) were determined.

2.4. Water vapour sorption

Sorption measurements were performed on 18 samples selected from decay test 1: decayed samples (weeks 1-5, N = 3) and control samples (week 1, N = 3). The samples were individually re-wrapped in plastic after the LFNMR measurements and stored at −20 °C until measurement in the automated sorption balance (Vsorp Enhanced, ProUmid, Germany). The sorption measurements were performed as described previously (Belt and Altgen, 2025), except that the samples were not water-saturated; instead, they were measured immediately after reaching room temperature by exposing the wrapped samples to ambient conditions. The samples were first measured in desorption by decreasing the relative humidity (RH) from 90% to 0% in 10% steps, followed by measurement in absorption using the same RH steps in the reverse order. The temperature was maintained at 25 °C. The mass of each sample was recorded at 15-min intervals. Each RH step was held until the change in sample mass was less than 0.01% for all samples, calculated from the slope of a linear regression line within a 60-min time window that advanced with each weighing step. The average sample mass within this moving time window was used as the reference mass. Finally, the dry mass was determined after exposing the samples to 40 °C and 0% RH for 48 h. Details on the mass stability of the sorption balance are provided by Belt and Altgen (2025).

2.5. Mass loss and moisture content

The decayed and control samples were dried after LFNMR and sorption measurements (overnight at room temperature, 24 h at 105 °C) to provide the final sample mass for mass loss and moisture content calculations. The mass of the fungal mycelium present in the decayed samples was not determined, which results in an overestimation of the final sample mass.

Mass loss (ML) due to decay was calculated for every sample according to Equation (1),

$$ML\ (\%) = \frac{m_{init} - m_{final}}{m_{init}} \times 100\% \quad (1)$$

where m_{init} is the initial dry mass, and m_{final} is the final, decayed dry mass.

Moisture contents were calculated on both a final, decayed mass basis (i.e., no correction for wood mass loss) and an initial, undecayed mass basis (i.e., corrected for mass loss). Moisture content (MC) and mass loss corrected moisture content (MC*) in the decaying state and water saturated state were calculated according to Equations (2) and (3),

$$MC\ (\%) = \frac{m_{wet} - m_{final}}{m_{final}} \times 100\% \quad (2)$$

$$MC^*\ (\%) = \frac{m_{wet} - m_{final}}{m_{init}} \times 100\% \quad (3)$$

where m_{wet} is the wet mass in the decaying state or the water saturated state, m_{final} is the final, decayed dry mass, m_{init} is the initial, undecayed dry mass.

From the LFNMR data, MC and MC* corresponding to the different LFNMR water populations (MC_i and MC_i*, respectively) were calculated according to Equations (4) and (5) as in previous studies (e.g. Beck et al., 2018b),

$$MC_i\ (\%) = \frac{A_i}{A_{total}} \times MC \quad (4)$$

$$MC_i^*\ (\%) = \frac{A_i}{A_{total}} \times MC^* \quad (5)$$

where A_i is the LFNMR peak area of a given water population, A_{total} is the total LFNMR peak area of all peaks, MC is moisture content in the decaying or water saturated state, and MC* is the mass loss corrected moisture content in the decaying or water saturated state.

Finally, from the sorption data, MC and MC* at different RH during the sorption measurement (MC_{RH} and MC_{RH}*, respectively) were calculated according to Equations (6) and (7),

$$MC_{RH}\ (\%) = \frac{m_{RH} - m_{final}}{m_{final}} \times 100\% \quad (6)$$

$$MC_{RH}^*\ (\%) = \frac{m_{RH} - m_{final}}{m_{init}} \times 100\% \quad (7)$$

where m_{RH} is the average sample mass during the final hour of each RH step, m_{final} is the final, decayed dry mass, m_{init} is the initial dry mass.

2.6. Compression strength

Compression strength was measured as an additional indicator for wood decay, given that decay fungi can cause significant strength loss at low mass losses (Witomski et al., 2016). The compression strength measurements were performed on all decayed samples from decay test 1 (weeks 1-5, N = 10) using the universal material testing machine Zwick Z050 (ZwickRoell, Germany). The samples were conditioned for 10 days in a conditioning chamber 65 ± 3 RH % and 20 ± 2 °C until the mass difference between two consecutive daily measurements was less than 0.2%. Before the compression test, the diameter of the specimens was measured with a calliper (accuracy of 0.01 mm) as the average of the diameters in two directions intersecting each other. The loading of force was done in the longitudinal direction at a steady speed of 2 mm/min, causing the test specimens to break within 0.5–1 min. The compression strength of a specimen at 12% moisture content (σ_{12}) was calculated according to Equation (8),

$$\sigma_{12}\ (Pa) = \frac{F_{max}}{A} \quad (8)$$

where F_{max} is the maximum load (N) and A is the compression area (mm^2).

2.7. Statistical analysis

Data on mass loss and moisture content obtained from the decayed wood samples were analysed using Welch's ANOVA with Games-Howell

post hoc test for pairwise comparisons (α = 5 %). The data were grouped based on the harvesting time (1, 2, 3, 4, and 5 weeks), and analyses were conducted separately for decay tests 1 and 2. All statistical analyses were performed using Minitab (Version 21.4, Minitab LLC, USA).

3. Results and discussion

3.1. Decay progression

The average mass losses caused by *C. puteana* over 5 weeks of incubation in decay tests 1 and 2 are shown in Fig. 2. *C. puteana* colonised the samples within a few days in both tests, but no mass loss was measured over the first two weeks in either test. The average mass losses became positive after three weeks of incubation: the average mass loss in test 1 was only 1%, while the average mass loss in test 2 reached 8%. Mass loss increased after four weeks of incubation, reaching 19% in test 1 and 16% in test 2. The samples from test 1 showed only a small increase in mass loss from week 4 to week 5, whereas the samples from test 2 showed a large increase to a final average mass loss of 46%. The average mass losses of the controls (Supplementary Fig. S2a) did not exceed 1.5% and showed no consistent change over the course of incubation.

The decaying state moisture contents of the samples are shown in Fig. 3a–b as a function of time and in Fig. 3c–d as a function of mass loss using both uncorrected (MC) and mass loss corrected (MC*) moisture content. The MCs of the sterile controls are shown in Supplementary Fig. S2b. In both decay tests, moisture content showed a substantial increase in the early stages of decay. In test 1, the average MC reached 63% after one week, while in test 2, the MC reached 102%. The average MC of the sterile controls did not exceed 30% after one week, which shows that a substantial portion of the water in the samples was derived from fungal activity. In test 1, the average MC increased to a maximum of 101% at week 3 and then decreased, while in test 2, the MC fluctuated between 102 and 86%. Plotting the individual MCs as a function of mass loss revealed a rapid increase in MC before mass loss in the test 1 samples, followed by a slight decrease with increasing mass loss. The test 2 samples showed no change in MC with mass loss. Using MC* instead of MC gives a different view of moisture in decaying wood because it eliminates any increase in MC caused by the decrease in sample mass. The MC* data revealed that the absolute amount of moisture in the samples decreased over time and as a function of mass loss. The decrease in MC* as a function of mass loss followed the same trend in test 1 and test 2. The MC of the sterile controls either increased slightly to a maximum of 40% (test 1, primarily due to condensation droplets) or stayed constant at approx. 26% (test 2) over time, which shows that the moisture changes in the decay test samples are due to fungal activity.

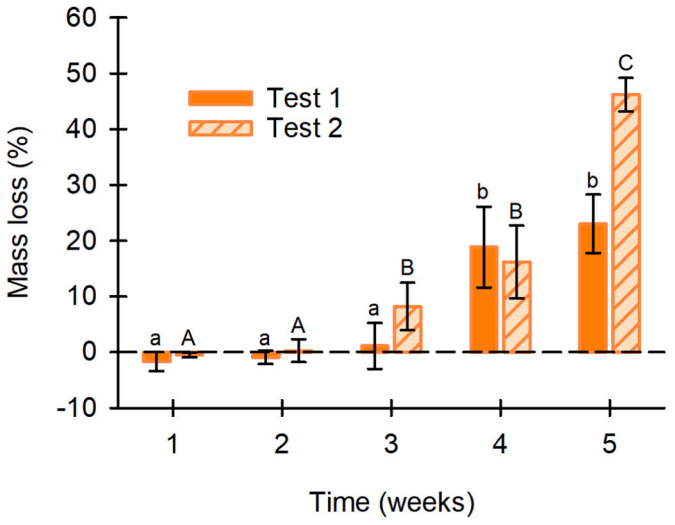

Fig. 2. Average (N = 10) mass loss due to *C. puteana* as a function of time in decay tests 1 and 2. Error bars are ±standard deviation. Different letters indicate a statistically significant difference (α = 5 %) in average (small letters for test 1, capital letters for test 2).

The moisture content results from the two time-series tests are unexpected, as it is usually believed that moisture content increases with decay. Moisture content is thought to increase during decay because fungi transport water into wood when a water source is available (Meyer and Brischke, 2015; Stienen et al., 2014) and because fungal respiration/carbohydrate breakdown generates water (Thybring, 2017). However, little data are available from time-series experiments. Our data show that moisture content does not necessarily increase with decay; it can, in fact, decrease, particularly when plotted using MC*. In our two decay tests, *C. puteana* transported water into the samples as evidenced by the much higher MC/MC* of the exposed samples than the sterile controls, in agreement with previous knowledge. However, in this experiment, the transport took place early in the decay process. Although moisture content peaked at different times in test 1 and test 2, the peak was reached before measurable mass loss in both tests. The fact that the initial increase in moisture content is a part of the incipient decay process becomes evident when MC* is plotted as a function of compression strength, which was measured for the test 1 samples (Supplementary Fig. S3). Brown rot degradation is known to affect mechanical properties more rapidly than mass loss (Witomski et al., 2016), and it can be seen that the initial increase in MC* takes place in incipient decay where strength has begun to decrease but mass loss is yet to start. The subsequent decrease in MC* with mass loss or strength loss suggests that water either evaporates, is consumed, or is transported out of the wood during the decay process.

3.2. Bound and free water dynamics

3.2.1. LFNMR water populations

Water populations in the decaying and control samples were investigated in the decaying state (decay tests 1 and 2) and the water-saturated state (decay test 2) using LFNMR. Example LFNMR T_2 distributions of one sterile control sample, one decayed sample with 14% mass loss, and one decayed sample with 49% mass loss in the decaying state and at full water saturation are shown in Fig. 4. All measured LFNMR T_2 distributions in the decaying state and saturated state are given in Supplementary Figs. S4 and S5, respectively. All decayed and control samples were found to have one to three peaks on their LFNMR distributions, depending on the sample and the measurement condition. The peaks were labelled 1-3 and assigned to bound water in cell walls (peak 1) and to free water outside cell walls (peaks 2 and 3) based on previous works (Araujo et al., 1992; Fredriksson and Thygesen, 2017; Telkki et al., 2013). In mature spruce, peak 2 has been assigned to water in pits, while peak 3 has been assigned to water in tracheid lumens, lumen ends, and ray lumens (Fredriksson and Thygesen, 2017). The decaying samples also contain fungal mycelium and water associated with it, but given the lack of data on mycelium-associated water, all LFNMR peak assignments were made and are interpreted assuming that the samples comprise only wood and water.

In the decaying state, the sterile control samples had one or two peaks on their LFNMR distributions. Most controls had only one peak, indicating that they contained only bound water. The decayed samples in turn had two or three peaks on their decaying state distributions, which shows that the samples contained free water in addition to bound water, as expected based on their moisture contents (Fig. 3). Most of the samples had only two peaks, likely because free water populations in different environments had similar T_2 times and were not resolved at moisture contents below saturation. A similar effect has been documented in water-saturated spruce latewood, where the relaxation component typically associated with peak 2 was not observable when the LFNMR data were processed by continuous curve-fit (Fredriksson

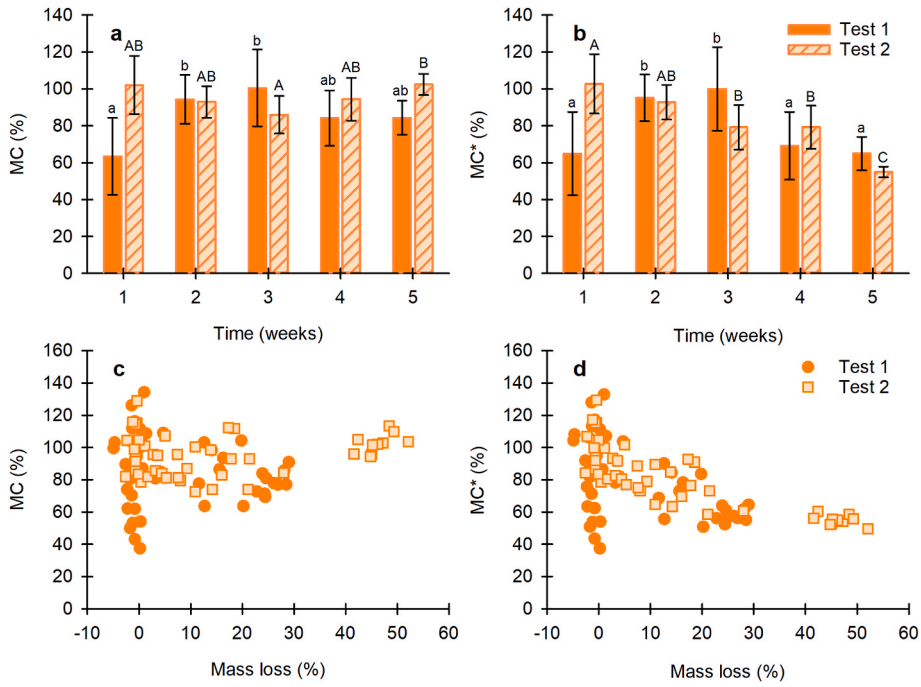

Fig. 3. Average (N = 10) MC (a) and MC* (b) as a function of time, and MC (c) and MC* (d) as a function of mass loss due to *C. puteana* in decay test 1 and 2. Error bars in a and b are ±standard deviation. Different letters indicate a statistically significant difference (α = 5 %) in average (small letters for test 1, capital letters for test 2). MC is moisture content, MC* is mass loss corrected moisture content.

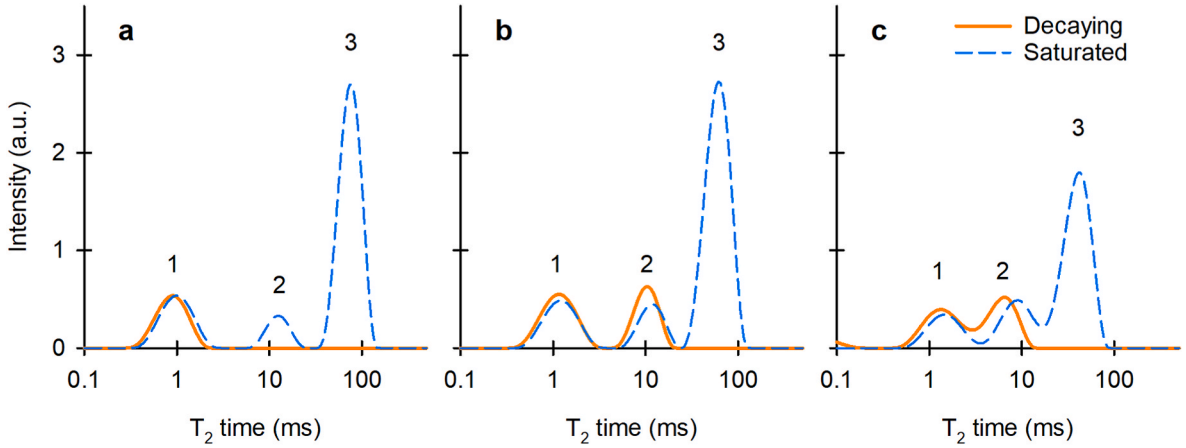

Fig. 4. Example LFNMR T_2 distributions of one control sample (a), one decayed sample with 14% mass loss (b), and one decayed sample with 49% mass loss (c) from decay test 2 in the decaying state and at full water saturation.

and Thygesen, 2017). At high mass losses, the free water peak(s) on the decayed samples appeared close to the bound water peak due to an increase in peak 1 T_2 time and a decrease in peak 2/peak 3 T_2 time. In the saturated state, all control and decayed samples had three peaks on their LFNMR distributions. The control samples exhibited three distinct peaks. However, as mass loss increased in the decayed samples, the corresponding T_2 components shifted toward one another and became increasingly difficult to resolve within the continuous LFNMR distributions.

3.2.2. *Bound and free water content*

Potential decay-induced changes in bound and free water content were investigated by analysing changes in peak areas (peak 1 for bound water, peak 2 + peak 3 for free water). The samples were first analysed in the decaying state to understand how *C. puteana* influences bound and free water content over the course of decay. Fig. 5a–b give peak areas as a function of decaying state MC*, while Fig. 5c–f give bound and free moisture contents (MC_{bound}, MC_{free}, MC_{bound}*, MC_{free}*) as a function of mass loss. Peak 1 area was not affected by decaying MC* above ca. 30%, while peak 2 + peak 3 area increased linearly with MC* above ca. 30%. The samples from test 2 had lower peak areas due to their smaller mass compared to the test 1 samples. When plotted as a function of mass loss, both MC_{bound} and MC_{bound}* increased slightly before measurable mass loss, indicating a small increase in bound water in incipient decay. MC_{bound} then increased with increasing mass loss, while MC_{bound}* stayed constant (test 1) or decreased slightly at high mass losses (test 2). MC_{free} and MC_{free}* increased before measurable mass loss and then decreased with mass loss; MC_{free}*followed the same pattern as decaying MC*, as expected given the clear relationship between MC* and peak 2 + peak 3 area.

In the decaying state, the relationships between peak areas and MC* were as expected and in agreement with previous works (Almeida et al.,

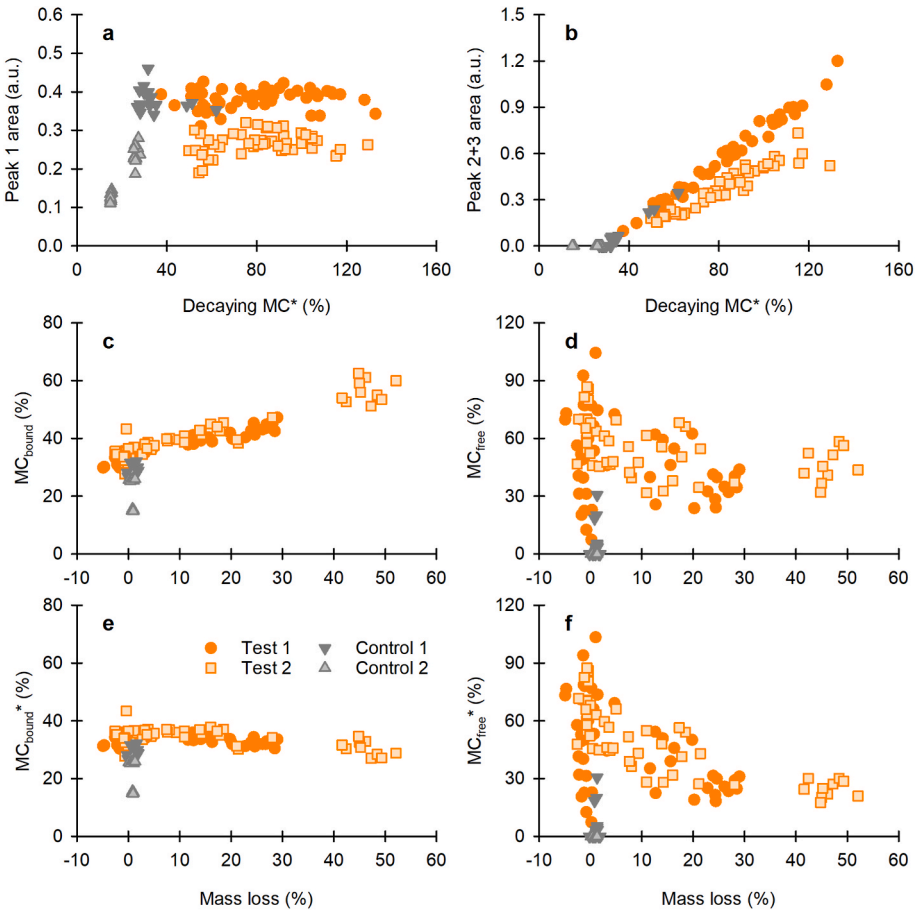

Fig. 5. T_2 peak areas of peak 1 (a) and peak 2 + peak 3 (b) as a function of decaying MC*, and MC_{bound} (c), MC_{free} (d), MC_{bound}* (e) and MC_{free}* (f) as a function of mass loss in decayed and control samples from decay tests 1 and 2 in the decaying state. MC is moisture content, MC* is mass loss corrected moisture content.

2007; Cox et al., 2010; Fredriksson et al., 2024; Sun et al., 2024). MC_{bound} increased with mass loss, indicating that degradation increased the relative amount of bound water held by the remaining cell wall material. The increase in MC_{bound} was expected, given that the selective removal of carbohydrates from the cell wall during brown rot decay is expected to create new cell wall space (Thybring, 2017). However, MC_{bound} did not increase at the rate expected if all the lost cell wall mass were replaced entirely with water (see Supplementary Fig. S6a). MC_{bound} increased at approximately the expected rate in early decay, but the rate of increase fell behind after ca. 10-20% mass loss (Supplementary Fig. S6b). MC_{bound}* in turn did not increase or even decreased with mass loss (Fig. 5e), indicating that there was no increase in absolute bound water content. The fact that MC_{bound}* did not increase with mass loss is surprising, since previous research conducted using the brown rot fungus *Rhodonia placenta* has revealed an increase in cell wall water-holding capacity on an absolute basis throughout decay in sweetgum (Flournoy et al., 1991) or at least in the early stages of decay in Scots pine (Belt and Altgen, 2025). However, the previous studies measured samples at full saturation rather than in the decaying state.

To gain further insight into water-holding capacity, the samples from decay test 2 were also analysed in the water-saturated condition. Fig. 6a–b shows peak areas as a function of saturation MC*, while Fig. 6c–f shows bound and free moisture contents (MC_{bound}, MC_{free}, MC_{bound}*, MC_{free}*) as a function of mass loss. Surprisingly, both peak 1 area and peak 2 + peak 3 area were only slightly influenced by saturation MC*. Peak 1 area increased slightly with saturation MC* in the decayed samples and decreased in the controls, while peak 2 + peak 3 area increased slightly in both sample types. Plotting the total peak area (peaks 1-3) of all decaying and saturated state measurements as a function of decaying/saturated MC* showed that total peak area increased until ca. 150% MC* and then plateaued (Supplementary Fig. S7a). However, the LFNMR signal was not saturated in even the highest MC* samples (Supplementary Fig. S7b), which suggests that other factors are responsible for the effect. When plotted as a function of mass loss, MC_{bound} and MC_{free} increased, although the variation in the MC_{bound} data in particular was high. MC_{bound}* in turn decreased at high mass loss, while MC_{free}* first increased and then decreased with mass loss.

Like the decaying state results, the saturated state measurements revealed that bound water content increased with decay on a decayed mass basis. However, as in the decaying state, saturation MC_{bound} increased at a slower rate than expected (Supplementary Fig. S6), and MC_{bound}* decreased rather than increased. The saturation results demonstrate that the surprising bound water findings seen in the decaying state are not just due to unexpected behaviour in non-saturated samples. The result partially contrasts previous findings (Belt and Altgen, 2025; Flournoy et al., 1991), and while the use of different experimental methods in the current and previous studies may play a role, it likely reflects real differences in cell wall degradation. Brown rot fungi typically utilise a diffusible mechanism rather than cell wall erosion or cavitation to remove carbohydrates from the cell wall (Arantes and Goodell, 2014; Goodell et al., 2017), increasing cell wall pore size and water-holding capacity. The creation of new water-accessible space might be reduced if a non-diffusive mechanism degrades the cell walls or if the space collapses after forming, explaining the lower-than-expected increase in MC_{bound} and the decrease in MC_{bound}*. The MC_{free}* trends (Fig. 6f) indicate that both mechanisms may be involved to some extent. The fact that MC_{free}* increased in early decay suggests that degradation

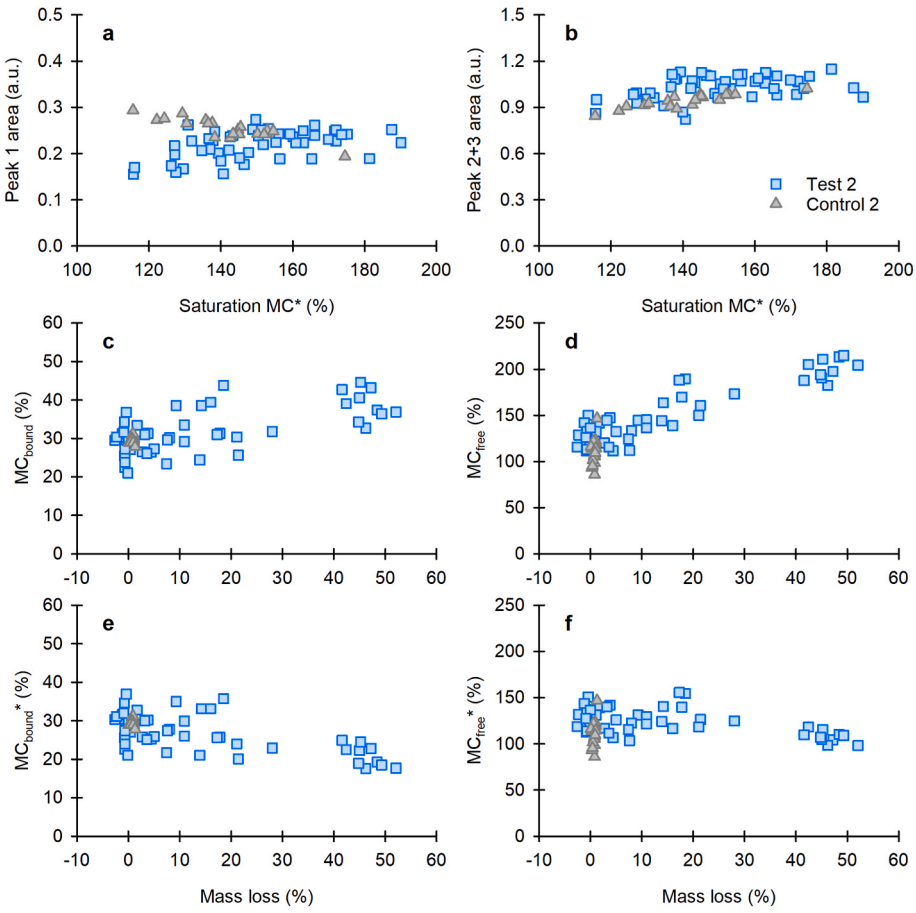

Fig. 6. T_2 peak areas of peak 1 (a) and peak 2 + peak 3 (b) as a function of saturation MC*, and MC_{bound} (c), MC_{free} (d), MC_{bound}* (e) and MC_{free}* (f) as a function of mass loss in decayed and control samples from decay test 2 in the saturated state. MC is moisture content, MC* is mass loss corrected moisture content.

increased the macropore volume in the samples, most likely due to the loss of cell wall volume. Although *C. puteana* often degrades wood using

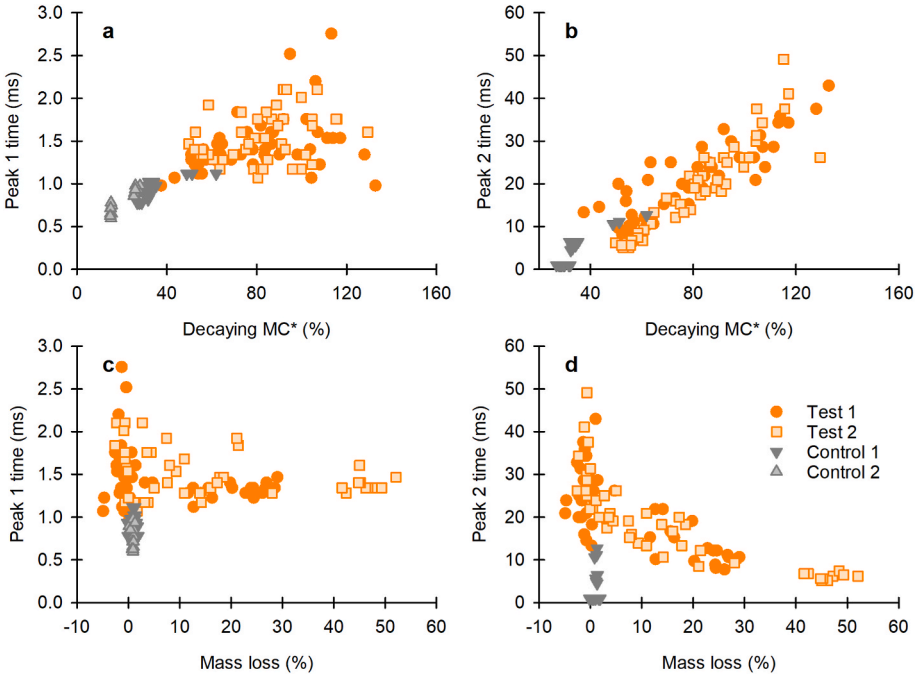

Fig. 7. T_2 peak times of peak 1 (a, c) and peak 2 (b, d) as a function of decaying MC* (a, b) and mass loss (c, d) in decayed and control samples from decay tests 1 and 2 in the decaying state. Smoothing parameter α set to 10.

the typical diffusible brown rot mechanism, degradation patterns involving cell wall erosion (Lee et al., 2004) and cavity formation (Kleist and Schmitt, 2001) have been detected. The fact that MC_{free}* then decreased in advanced decay suggests that the samples underwent a decrease in macropore volume, most likely due to shrinkage. There was a visible decrease in external sample dimensions in advanced decay, which also suggests shrinkage.

3.2.3. Chemical and physical environment

In LFNMR, the different water populations are not only characterised by their peak areas but also by their peak times, which are influenced by the chemical and physical characteristics of the substrate (Beck et al., 2018a, 2018b; Fredriksson et al., 2024; Thygesen and Elder, 2008; Yang et al., 2020). Peak times were first analysed in the decaying state to understand how *C. puteana* changes wood-water interactions over the course of decay. Fig. 7 shows the T_2 times of the bound water peak (peak 1) and the free water peak with the longest relaxation time (peak 2 for most samples and peak 3 for three samples that had three peaks on their distribution) as a function of decaying MC* and mass loss. Peak 1 time increased with decaying MC* until ca. 40-50% MC*, after which data variation increased dramatically, and no clear trends could be identified. Peak 2 time in turn increased with decaying MC*. The samples from test 1 were split into two separate populations at lower MCs*, with the week 1 samples showing higher T_2 times than the more extensively decayed samples from weeks 4 and 5. The samples from decay test 2 showed a linear relationship between peak 2 time and MC* that aligned with the more extensively degraded samples from decay test 1. Peak 1 time also showed considerable variation as a function of mass loss, with no correlation observed. Peak 2 time first increased before measurable mass loss and then decreased, following a similar pattern as decaying MC* (Fig. 3); however, peak 2 time decreased faster than decaying MC* as a function of mass loss.

The decaying state results showed that peak times were primarily influenced by decaying MC* with a lesser influence from mass loss. The influence of MC* on peak times is in line with previous works (Almeida et al., 2007; Cox et al., 2010; Sun et al., 2024). Mass loss had no obvious effect on peak 1 time, while peak 2 time decreased as a result of mass loss. T_2 peak times decrease when wood-water interactions become stronger, as a result of reduced pore size or increased hygroscopicity (Beck et al., 2018b; Fredriksson et al., 2024; Thygesen and Elder, 2008; Yang et al., 2020). The decrease in peak 2 time is most likely primarily due to increased hygroscopicity in the decaying state, as demonstrated in previous experiments (Belt et al., 2024; Belt and Altgen, 2025). The hygroscopicity increase may be related to degradative changes in the wood cell wall polymers (Belt et al., 2024) or to the accumulation of soluble carbohydrate fragments, which have been shown to decrease T_2 peak times in LFNMR (Hsieh et al., 2014). Decreased pore size is unlikely to play a role, at least until advanced decay stages. The saturation MC_{free}* trends (Fig. 6f) indicated that there was a decrease in pore volume in the late stages of decay due to shrinkage, which may be associated with a reduction in pore size.

Peak times were also analysed in the saturated state. The T_2 times of peaks 1-3 in the saturated decay test 2 samples are shown in Fig. 8 as a function of saturation MC* and mass loss. All peak times showed high variation when plotted as a function of saturation MC*. As expected, peak 1 time did not correlate with saturation MC*, while peak 2 and peak 3 times increased with saturation MC*. The peak 3 times separated the decayed and control samples into different populations, with the controls showing higher peak times than the decayed samples. When plotted as a function of mass loss, peak 1 time showed very high variation, making trends difficult to analyse. Peak 2 and peak 3 times in turn decreased with mass loss. There was a clear decrease in peak 2 and peak

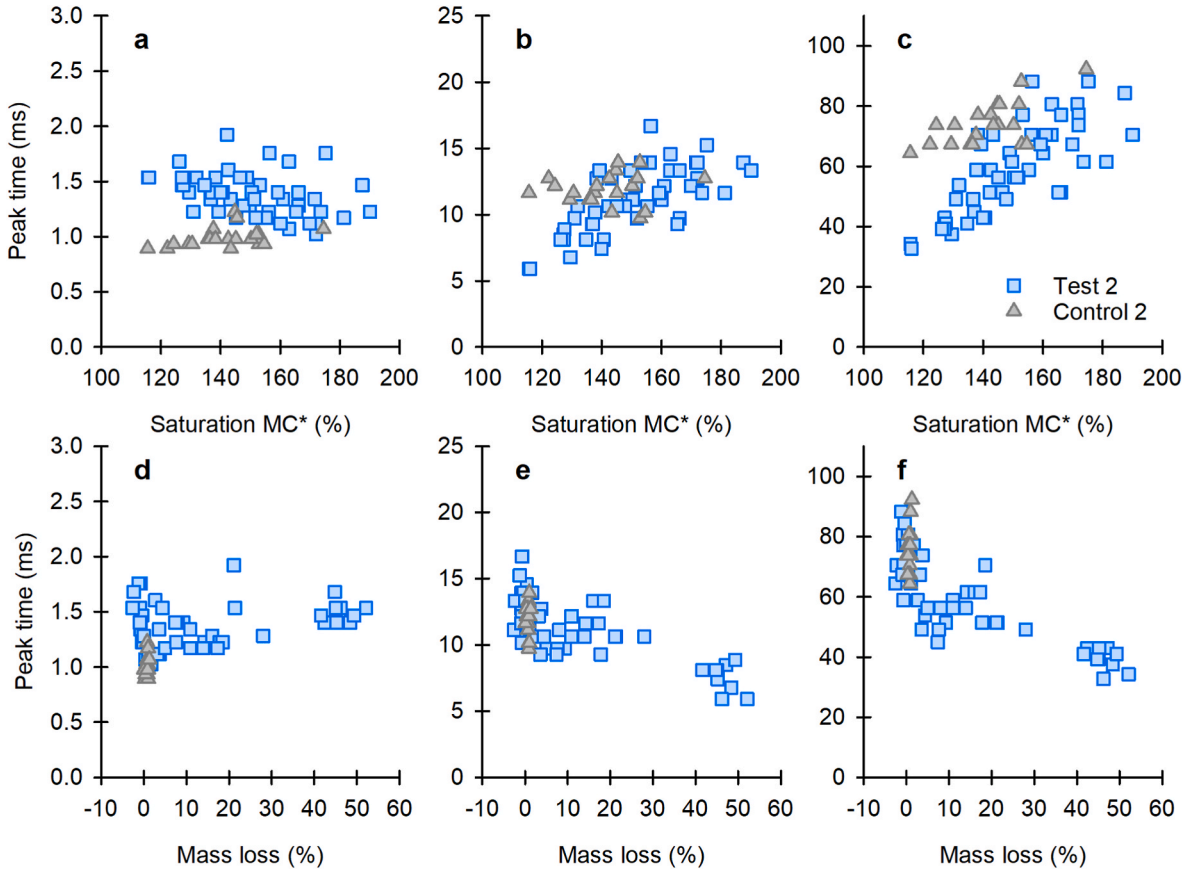

Fig. 8. T_2 peak times of peak 1 (a, d), peak 2 (b, e), and peak 3 (c, f) as a function of saturation MC* (a-c) and mass loss (d-f) in decayed and control samples from decay test 2 in the water saturated state. Smoothing parameter α set to 10.

3 time in early decay (<5% mass loss) and advanced decay (>40% mass loss). At intermediate decay stages, the peak times increased and then decreased. The increase in peak 2 and peak 3 times at ca. 20% mass loss is most likely due to the increase in MC_{free}* (Fig. 6f) at this stage of decay.

The saturation measurements were unable to reveal clear trends in peak 1 time development, but the results confirm a decrease in free water peak times with increasing mass loss. The results contrast previous LFNMR findings on brown rot decayed wood, which found an increase in peak 1 and no change in peak 2 or peak 3 time with *R. placenta* mass loss in unmodified Scots pine in the saturated state (Beck et al., 2018a). Beck et al. assigned the increase in peak 1 time to an increase in porosity, and the lack of increase in the current experiment may be due to the lower-than-expected increase in water-accessible cell wall space. However, it is also possible that the high data variation masks the increase in peak 1 time. The differences in peak 2 and peak 3 time trends between the previous and current results may, in turn, be due to leaching. An extensive leaching procedure was applied by Beck et al., while the current samples were only soaked for less than two days with no water changes. The current samples are therefore still likely to contain hydrophilic degradation products, which may contribute to the decrease in peak 2 and peak 3 times.

3.3. Hygroscopicity

Finally, a subset of samples from decay test 1 was used for sorption measurements to understand the relationship between water in decaying wood and decay-induced changes in hygroscopicity. The sorption isotherms were measured on undried samples starting in desorption from the decaying state, as before (Belt et al., 2024; Belt and Altgen, 2025), except that water saturation before measurement was omitted. Example isotherms of the most extensively decayed sample (29% mass loss) and one undecayed control sample are shown in Fig. 9a, while the moisture contents of all measured decayed and control samples at 90% RH in desorption and absorption ($MC_{90\%}$ and $MC_{90\%}$*) are shown in Fig. 9b–c as a function of mass loss. All sorption isotherms are shown in Supplementary Fig. S8. The isotherms showed that the decayed sample had increased MC at 90% RH and decreased MC at RHs below 90% in both desorption and absorption relative to the control sample. The findings are partially in agreement with previous results, which found an increase in MC at 90% RH in desorption but no increase at any RH in absorption in Scots pine sapwood degraded by *C. puteana* (Belt et al., 2024) and *R. placenta* (Belt et al., 2024; Belt and Altgen, 2025). When $MC_{90\%}$ were plotted against mass loss (Fig. 9b), the desorption MCs showed a clear progressive increase with mass loss as before. The absorption MCs also increased slightly, in contrast to the decrease seen before (Belt et al., 2024; Belt and Altgen, 2025). $MC_{90\%}$*, on the other hand, showed a clear decrease with mass loss in both desorption and absorption. The decayed samples had higher $MC_{90\%}$* than the controls at low mass losses, particularly in desorption, but the values decreased below the control values with increasing mass loss.

The sorption measurements showed that *C. puteana* degradation changed the hygroscopicity of the wood. Hygroscopicity increased before measurable mass loss, as evidenced by the higher $MC_{90\%}$ and $MC_{90\%}$* of the exposed samples compared to the sterile controls. The increasing $MC_{90\%}$ then showed that the hygroscopicity of the remaining cell wall material continued to increase with mass loss. However, the decrease in $MC_{90\%}$* showed that the absolute amount of moisture in the samples decreased with increasing decay, as expected given the loss of moisture-absorbing cell wall material. The causes of the increase in hygroscopicity remain unclear, but both physical and chemical factors may play a role. The increased hygroscopicity of the remaining cell wall material agrees with the decrease in peak 2 and peak 3 times seen in the decaying and saturated states (Figs. 7 and 8); however, other factors may also contribute to the decrease in free water peak times. The increased hygroscopicity is also consistent with the increase in MC_{bound} (Fig. 5c). Still, it is clear that hygroscopicity is not a critical factor in controlling the overall moisture dynamics during decay. The rapid initial increase and subsequent gradual decrease in decaying MC* (Fig. 3d) cannot be attributed to the changes in hygroscopicity.

Overall, our results revealed surprising moisture dynamics in wood degraded by *C. puteana*, demonstrating that wood decay can affect water in wood in ways that go against common expectations. However, our results should not be generalised but rather taken as a call for more studies into moisture dynamics during wood decay. Moisture dynamics should be investigated in different test setups and in different fungal species to explore the influence of environmental conditions and fungal biology – further studies should also be conducted using *C. puteana* to understand the effects of potential variations in cell wall degradation mechanisms. A better understanding of moisture dynamics during wood decay will be important for protecting wood in service and for predicting the service life of wooden construction.

4. Conclusions

Our time-series decay tests revealed that gravimetric MC* decreased

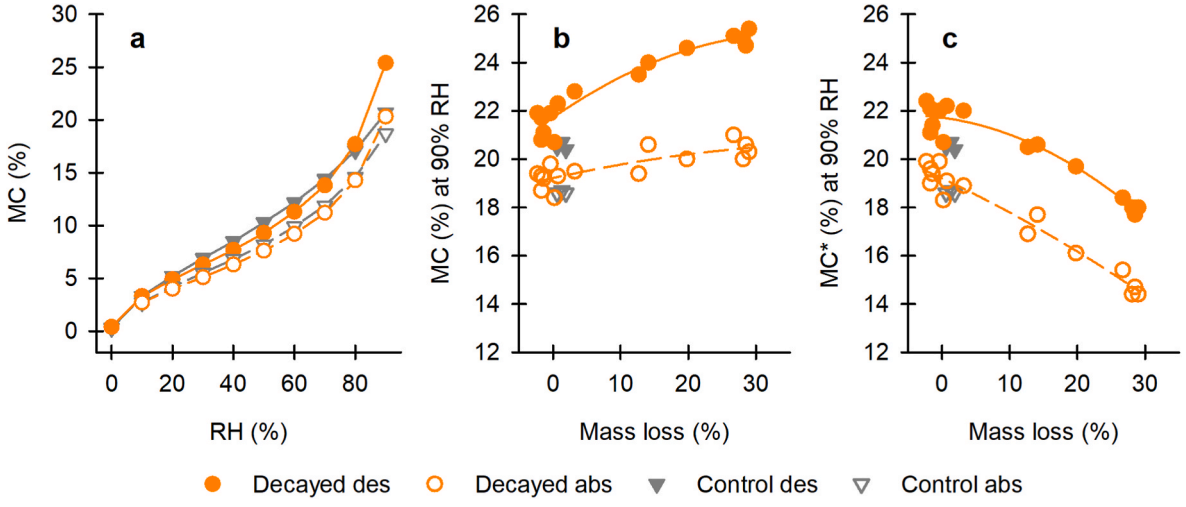

Fig. 9. Sorption isotherms of one decayed sample (29% mass loss) and one control sample in desorption from the undried decaying state and in absorption from the dried state (a), and MC (b) and MC* (c) of all measured decayed and control samples at 90% RH in desorption and absorption as a function of mass loss. MC is moisture content, MC* is mass loss corrected moisture content.

rather than increased with decay; the only increase in MC* occurred in early decay before measurable mass loss. MC_{bound} increased with mass loss in the decaying state and water-saturated state, indicating that the amount of bound water held by the remaining wood material increased. However, MC_{bound} increased less than expected, and there was no increase in the mass loss-corrected MC_{bound}*. The lack of increase in water-accessible cell wall space suggests that *C. puteana* may have degraded the wood samples by an atypical brown rot mechanism or that the samples may have undergone shrinkage following carbohydrate removal. The MC_{free}* results obtained in the saturated state suggest that both mechanisms may play a role. *C. puteana* degradation caused changes in hygroscopicity, but the changes were not a critical factor in determining the moisture content of wood during decay.

CRediT authorship contribution statement

Tiina Belt: Writing – review & editing, Writing – original draft, Visualization, Resources, Methodology, Investigation, Funding acquisition, Conceptualization. **Andreas Treu:** Writing – review & editing, Validation, Formal analysis. **Veikko Möttönen:** Writing – review & editing, Investigation. **Michael Altgen:** Writing – review & editing, Investigation, Formal analysis, Conceptualization.

Declaration of competing interest

The authors declare that they have no known competing financial interests or personal relationships that could have appeared to influence the work reported in this paper.

Acknowledgements

This work was supported by the Research Council of Finland (grant number 349198) and by the Research Council of Norway (Contract No. 342631).

Appendix A. Supplementary data

Supplementary data to this article can be found online at https://doi.org/10.1016/j.ibiod.2026.106296.

Data availability

The datasets generated during the current study are available in the Zenodo repository at doi.org/10.5281/zenodo.16946361.

References

Almeida, G., Gagné, S., Hernández, R.E., 2007. A NMR study of water distribution in hardwoods at several equilibrium moisture contents. Wood Sci. Technol. 41, 293–307. https://doi.org/10.1007/s00226-006-0116-3.

Arantes, V., Goodell, B., 2014. Current understanding of brown-rot fungal biodegradation mechanisms: a review. In: Deterioration and Protection of Sustainable Biomaterials, ACS Symposium Series. American Chemical Society, pp. 3–21. https://doi.org/10.1021/bk-2014-1158.ch001.

Araujo, C.D., MacKay, A.L., Hailey, J.R.T., Whittall, K.P., Le, H., 1992. Proton magnetic resonance techniques for characterization of water in wood: application to white spruce. Wood Sci. Technol. 26, 101–113. https://doi.org/10.1007/BF00194466.

Beck, G., Thybring, E.E., Thygesen, L.G., 2018a. Brown-rot fungal degradation and deacetylation of acetylated wood. Int. Biodeterior. Biodegrad. 135, 62–70. https://doi.org/10.1016/j.ibiod.2018.09.009.

Beck, G., Thybring, E.E., Thygesen, L.G., Hill, C., 2018b. Characterization of moisture in acetylated and propionylated radiata pine using low-field nuclear magnetic resonance (LFNMR) relaxometry. Holzforschung 72, 225–233. https://doi.org/10.1515/hf-2017-0072.

Belt, T., Altgen, M., 2025. Changes in wood-water relations in acetylated wood over the course of Rhodonia placenta brown rot decay. J. Mater. Sci. Mater. Electron. 20, 19. https://doi.org/10.1186/s40712-025-00228-5.

Belt, T., Altgen, M., Awais, M., Nopens, M., Rautkari, L., 2024. Degradation by brown rot fungi increases the hygroscopicity of heat-treated wood. Int. Biodeterior. Biodegrad. 186, 105690. https://doi.org/10.1016/j.ibiod.2023.105690.

Bonnet, M., Courtier-Murias, D., Faure, P., Rodts, S., Care, S., 2017. NMR determination of sorption isotherms in earlywood and latewood of Douglas fir. Identification of bound water components related to their local environment. Holzforschung 71, 481–490. https://doi.org/10.1515/hf-2016-0152.

Brischke, C., Alfredsen, G., 2020. Wood-water relationships and their role for wood susceptibility to fungal decay. Appl. Microbiol. Biotechnol. 104, 3781–3795. https://doi.org/10.1007/s00253-020-10479-1.

Brischke, C., Soetbeer, A., Meyer-Veltrup, L., 2017. The minimum moisture threshold for wood decay by basidiomycetes revisited. A review and modified pile experiments with Norway spruce and European beech decayed by Coniophora puteana and Trametes versicolor. Holzforschung 71, 893–903. https://doi.org/10.1515/hf-2017-0051.

Cardias, M. de F.C., 1992. The Protection of Wood Against Fungal Decay by Isocyanate Chemical Modification (Doctoral Dissertation). Bangor University.

Cardias Williams, F., Hale, M.D., 2003. The resistance of wood chemically modified with isocyanates: the role of moisture content in decay suppression. Int. Biodeterior. Biodegrad. 52, 215–221. https://doi.org/10.1016/S0964-8305(03)00070-2.

Carr, H.Y., Purcell, E.M., 1954. Effects of diffusion on free precession in nuclear magnetic resonance experiments. Phys. Rev. 94, 630–638. https://doi.org/10.1103/PhysRev.94.630.

Cox, J., McDonald, P.J., Gardiner, B.A., 2010. A study of water exchange in wood by means of 2D NMR relaxation correlation and exchange. Holzforschung 64, 259–266. https://doi.org/10.1515/hf.2010.036.

EN 350, 2016. Durability of wood and wood-based products. Testing and Classification of the Durability to Biological Agents of Wood and Wood-based Materials.

Flournoy, D.S., Kirk, T.K., Highley, T.L., 1991. Wood decay by brown-rot fungi: changes in pore structure and cell wall volume. Holzforschung 45, 383–388. https://doi.org/10.1515/hfsg.1991.45.5.383.

Fredriksson, M., 2019. On wood–water interactions in the over-hygroscopic moisture Range—Mechanisms, methods, and influence of wood modification. Forests 10, 779. https://doi.org/10.3390/f10090779.

Fredriksson, M., Digaitis, R., Engqvist, J., Thybring, E.E., 2024. Effect of targeted acetylation on wood–water interactions at high moisture states. Cellulose 31, 869–885. https://doi.org/10.1007/s10570-023-05678-8.

Fredriksson, M., Thybring, E.E., 2019. On sorption hysteresis in wood: separating hysteresis in cell wall water and capillary water in the full moisture range. PLoS One 14, e0225111. https://doi.org/10.1371/journal.pone.0225111.

Fredriksson, M., Thygesen, L.G., 2017. The states of water in Norway spruce (Picea abies (L.) Karst.) studied by low-field nuclear magnetic resonance (LFNMR) relaxometry: assignment of free-water populations based on quantitative wood anatomy. Holzforschung 71, 77–90. https://doi.org/10.1515/hf-2016-0044.

Gabriel, J., Švec, K., 2017. Occurrence of indoor wood decay basidiomycetes in Europe. Fungal Biol Rev 31, 212–217. https://doi.org/10.1016/j.fbr.2017.05.002.

Godefroy, S., Ryland, B., Callaghan, P.T., 2003. 2D Laplace Inversion Instruction Manual. Victoria University of Wellington, Wellington, New Zealand.

Goodell, B., Zhu, Y., Kim, S., Kafle, K., Eastwood, D., Daniel, G., Jellison, J., Yoshida, M., Groom, L., Pingali, S.V., O'Neill, H., 2017. Modification of the nanostructure of lignocellulose cell walls via a non-enzymatic lignocellulose deconstruction system in brown rot wood-decay fungi. Biotechnol. Biofuels 10, 179. https://doi.org/10.1186/s13068-017-0865-2.

Hiltunen, S., Mankinen, A., Javed, M.A., Ahola, S., Venäläinen, M., Telkki, V.-V., 2020. Characterization of the decay process of Scots pine caused by Coniophora puteana using NMR and MRI. Holzforschung 74, 1021–1032. https://doi.org/10.1515/hf-2019-0246.

Hsieh, C.C., Cannella, D., Jørgensen, H., Felby, C., Thygesen, L.G., 2014. Cellulase inhibition by high concentrations of monosaccharides. J. Agric. Food Chem. 62, 3800–3805. https://doi.org/10.1021/jf5012962.

Jakes, J.E., Hunt, C.G., Zelinka, S.L., Ciesielski, P.N., Plaza, N.Z., 2019. Effects of moisture on diffusion in unmodified wood cell walls: a phenomenological polymer science approach. Forests 10, 1084. https://doi.org/10.3390/f10121084.

Kleist, G., Schmitt, U., 2001. Characterisation of a soft rot-like decay pattern caused by Coniophora puteana (Schum.) Karst. in sapelli wood (Entandrophragma cylindricum sprague). Holzforschung 55, 573–578. https://doi.org/10.1515/HF.2001.093.

Lee, K.H., Wi, S.G., Singh, A.P., Kim, Y.S., 2004. Micromorphological characteristics of decayed wood and laccase produced by the brown-rot fungus Coniophora puteana. J. Wood Sci. 50, 281–284. https://doi.org/10.1007/s10086-003-0558-2.

Meiboom, S., Gill, D., 1958. Modified spin-echo method for measuring nuclear relaxation times. Rev. Sci. Instrum. 29, 688–691. https://doi.org/10.1063/1.1716296.

Meyer, L., Brischke, C., 2015. Fungal decay at different moisture levels of selected European-grown wood species. Int. Biodeterior. Biodegrad. 103, 23–29. https://doi.org/10.1016/j.ibiod.2015.04.009.

Müller, U., Bammer, R., Halmschlager, E., Stollberger, R., Wimmer, R., 2001. Detection of fungal wood decay using Magnetic Resonance Imaging. Holz Roh Werkst 59, 190–194. https://doi.org/10.1007/s001070100202.

Richter, H.G., Grosser, D., Heinz, I., Gasson, P.E., 2004. IAWA list of microscopic features for softwood identification. IAWA J. 25, 1–70. https://doi.org/10.1163/22941932-90000349.

Saito, H., Fukuda, K., Sawachi, T., 2012. Integration model of hygrothermal analysis with decay process for durability assessment of building envelopes. Build. Simulat. 5, 315–324. https://doi.org/10.1007/s12273-012-0081-8.

Schmidt, O., 2007. Indoor wood-decay basidiomycetes: damage, causal fungi, physiology, identification and characterization, prevention and control. Mycol. Prog. 6, 261. https://doi.org/10.1007/s11557-007-0534-0.

Stienen, T., Schmidt, O., Huckfeldt, T., 2014. Wood decay by indoor basidiomycetes at different moisture and temperature. Holzforschung 68, 9–15. https://doi.org/10.1515/hf-2013-0065.

Sun, F., Chen, K., Tan, Y., Peng, H., Zhan, T., Cai, L., Lyu, J., 2024. Characterization of stable and unstable states of moisture in wood during sorption by low-field NMR. Ind. Crops Prod. 210, 118109. https://doi.org/10.1016/j.indcrop.2024.118109.

Telkki, V.-V., Yliniemi, M., Jokisaari, J., 2013. Moisture in softwoods: fiber saturation point, hydroxyl site content, and the amount of micropores as determined from NMR relaxation time distributions. Holzforschung 67, 291–300. https://doi.org/10.1515/hf-2012-0057.

Thybring, E.E., 2017. Water relations in untreated and modified wood under brown-rot and white-rot decay. Int. Biodeterior. Biodegrad. 118, 134–142. https://doi.org/10.1016/j.ibiod.2017.01.034.

Thybring, E.E., Digaitis, R., Nord-Larsen, T., Beck, G., Fredriksson, M., 2020. How much water can wood cell walls hold? A triangulation approach to determine the maximum cell wall moisture content. PLoS One 15, e0238319. https://doi.org/10.1371/journal.pone.0238319.

Thygesen, L.G., Elder, T., 2008. Moisture in untreated, acetylated, and furfurylated Norway spruce studied during drying using time domain NMR. Wood Fiber Sci. 40, 309–320.

Viitanen, H., Toratti, T., Makkonen, L., Peuhkuri, R., Ojanen, T., Ruokolainen, L., Räisänen, J., 2010. Towards modelling of decay risk of wooden materials. Eur J Wood Prod 68, 303–313. https://doi.org/10.1007/s00107-010-0450-x.

Wimmers, G., 2017. Wood: a construction material for tall buildings. Nat. Rev. Mater. 2, 17051. https://doi.org/10.1038/natrevmats.2017.51.

Witomski, P., Olek, W., Bonarski, J.T., 2016. Changes in strength of Scots pine wood (*Pinus silvestris* L.) decayed by brown rot (*Coniophora puteana*) and white rot (*Trametes versicolor*). Constr. Build. Mater. 102, 162–166. https://doi.org/10.1016/j.conbuildmat.2015.10.109.

Yang, T., Thybring, E.E., Fredriksson, M., Ma, E., Cao, J., Digaitis, R., Thygesen, L.G., 2020. Effects of changes in biopolymer composition on moisture in acetylated wood. Forests 11, 719. https://doi.org/10.3390/f11070719.

Zabel, R.A., Morrell, J.J., 2020. Wood deterioration agents. In: Zabel, R.A., Morrell, J.J. (Eds.), Wood Microbiology - Decay and Its Prevention. Academic Press, San Diego, pp. 19–54. https://doi.org/10.1016/B978-0-12-819465-2.00002-4.